UC Irvine
UC Irvine Previously Published Works

Title
The Use of the Dimensionless Womersley Number to Characterize the Unsteady Nature of Internal Flow

Permalink
https://escholarship.org/uc/item/31422175

Journal
Journal of Theoretical Biology, 191(1)

ISSN
0022-5193

Authors
Loudon, Catherine
Tordesillas, Antoinette

Publication Date
1998-03-01

DOI
10.1006/jtbi.1997.0564

Peer reviewed

The Use of the Dimensionless Womersley Number to Characterize the Unsteady Nature of Internal Flow

Catherine Loudon*‡ and Antoinette Tordesillas†

Department of Entomology, University of Kansas, Lawrence, KS 66045 U.S.A.; †Department of Mathematics and Statistics, The University of Melbourne, Parkville, Victoria 3052, Australia

Dimensionless numbers are very useful in characterizing mechanical behavior because their magnitude can often be interpreted as the relative importance of competing forces that will influence mechanical behavior in different ways. One dimensionless number, the Womersley number (Wo), is sometimes used to describe the unsteady nature of fluid flow in response to an unsteady pressure gradient; i.e., whether the resulting fluid flow is quasi-steady or not. Fluids surround organisms which themselves contain fluid compartments; the behaviors exhibited by these biologically-important fluids (e.g. air, water, or blood) are physiologically significant because they will determine to a large extent the rates of mass and heat exchange and the force production between an organism and its environment or between different parts of an organism.

In the biological literature, the use of the Womersley number is usually confined to a single geometry: the case of flow inside a circular cylinder. We summarize the evidence for a broader role of the Womersley number in characterizing unsteady flow than indicated by this geometrical restriction. For the specific category of internal flow, we show that the exact analytical solution for unsteady flow between two parallel walls predicts the same pattern of fluid behavior identified earlier for flow inside cylinders; i.e., a dichotomy in fluid behavior for values of $Wo < 1$ and $Wo > 1$. When $Wo < 1$, the flow is predicted to faithfully track the oscillating pressure gradient, and the velocity profiles exhibit a parabolic shape such that the fluid oscillating with the greatest amplitude is farthest from the walls ("quasi-steady" behavior). When $Wo > 1$, the velocity profiles are no longer parabolic, and the flow is phase-shifted in time relative to the oscillating pressure gradient. The amplitude of the oscillating fluid may either increase or decrease as $Wo > 1$, as described in the text.
© 1998 Academic Press Limited

Introduction

Organisms live surrounded by fluids: air and water. In addition, organisms are filled with fluid compartments, such as circulatory systems or gastrovascular cavities (e.g. Vogel, 1992). The fluid flow adjacent to the external and internal body parts of organisms affects a great many important physiological functions, such as the rate of mass exchange between a body part and the surrounding fluid (e.g. oxygen uptake, nitrogenous waste release, or chemical signal interception), heat exchange, or the production of forces in locomotion (Denny, 1993; Vogel, 1994a). This fluid flow is frequently unsteady from the frame of reference of the body part; this can occur either because the flow is unsteady when it reaches a body part, or because the body parts themselves undergo oscillatory movements (Daniel, 1984; Vogel, 1994a).

Even a qualitative description of physiological function is greatly complicated by the consideration of unsteady influences, and therefore a common question is, when can the unsteady nature of the flow be safely ignored? Of course, the significance of

‡Author to whom correspondence should be addressed. E-mail: loudon@ukans.edu

unsteady flow goes beyond the potential inconvenience to the physiologist; unsteady flow may have unexpected or non-intuitive influences on function. The most dramatic illustration of this is probably the discovery of novel unsteady ways of generating lift by insect wings (Weis-Fogh, 1973; Ellington, 1984). Simple methods to evaluate aspects of the behavior of unsteady flow are thus of broad utility.

A dimensionless quantity that may serve as a general-purpose indicator of the nature of unsteady flow is the Womersley number, Wo,

$$Wo = \frac{L}{2}\sqrt{\frac{n}{v}} \qquad (1)$$

where L is the characteristic length in m; n is the frequency of the unsteady flow or movements in radians/s ($n = 2\pi f$ where f is frequency in cycles/s), and v is the kinematic viscosity of the fluid in m^2/s. At the present time this dimensionless parameter is used almost exclusively for cases of flow inside circular cylinders, at least in the biological literature (e.g. Pedley et al., 1977; Caro et al., 1978; Daniel et al., 1989; Vogel, 1994a), presumably because this is the geometry for which a mathematical foundation has been laid in an explicit biological context. Four decades ago such a foundation was laid in a study on flow in mammalian blood vessels (Womersley, 1955); this flow is unsteady because of the rhythmic nature of pressure applied by a beating heart. Womersley identified a dimensionless parameter group (equation 1, L = internal diameter of the cylindrical vessel), later named after him, useful in indicating a dichotomy in fluid behavior: when $Wo < 1$, the fluid behaves in a "quasi-steady" manner, while for $Wo > 1$, the behavior of the fluid deviates more and more from quasi-steady behavior. Note that this (standard) terminology can be confusing: "quasi-steady" does not mean "approximately steady" (i.e., not changing very much in time). Rather, "quasi-steady" means that at any time, the instantaneous flow rate is determined by the instantaneous pressure gradient. Thus, quasi-steady flow can actually oscillate *more* vigorously than non-quasi-steady flow simply because it will keep up with a rapidly changing pressure gradient. Womersley's contribution was evaluated by McDonald (1955, p. 547), who pointed out that there were "no theoretical innovations but it is original in that it is put in a form that can be computed easily" (this ease of computation assumes familiarity with Bessel functions and Fourier series). Parallel but separate mathematical treatments at that same time in the engineering literature may be

accessed by consulting Schlichting (1979) or White (1991).

The purpose of this study is to document the more general use of the Womersley number, i.e., for flow situations other than inside circular cylinders. In fluid mechanical terms, the fundamental importance of Wo is demonstrated by its appearance in non-dimensional forms of the fluid mechanical Navier–Stokes equations along with another dimensionless number, the Reynolds number (Re)

$$Re = \frac{LU_0}{v} \qquad (2)$$

where U_0 is a characteristic velocity [e.g. p. 54, Happel & Brenner (1965) the "vibrational Reynolds number" $L^2 n/v$ is used instead of Wo; or p. 131 in Fung (1997)]. Thus, if Re and Wo are the same for two geometrically similar flows, the flows are considered "dynamically similar" meaning that the (dimensionless) solutions for velocity are identical (Fung, 1997, p. 131) whether or not the solutions can be derived. Exact solutions of the Navier–Stokes equations for unsteady flow are possible only for very simple geometries or restricted boundary conditions.

In many biological applications an investigator may need only a qualitative indicator of fluid behavior. Because of its appearance in the Navier–Stokes equations, Wo is such a qualitative indicator for unsteady flow behavior. Before associations may be made between unsteady fluid behaviors and magnitudes of Wo, the appropriate foundation must be laid for the relevant physical setting (which will include the geometry and Re range).

To extend the present foundation for the application of Wo in an explicit biological context, we consider another case of internal flow. We provide the exact analytical solutions for the unsteady flow between two parallel walls that results from a sinusoidally-applied pressure gradient (solutions for velocity, volume flow rate, and velocity gradient at the wall). We report these solutions in a form more accessible to a broad biological audience than usually found in the fluid mechanical engineering literature, i.e., the solutions are not left in differential, integral, or complex form. While the direct applications of these mathematical solutions are restricted to cases of flow through gaps of appropriate geometry, the value of considering the general patterns of fluid behavior described by these equations is that these patterns will approximate the fluid behavior for many other geometries for which exact solutions are not available. We tabulate examples of dimensionless parameters similar to the Womersley number, primarily from the engineering literature, both to alert users to

differences in notation and definition and to underscore that the Womersley number is of more general applicability than currently recognized in the biological literature.

Mathematical Solutions for Internal Flow Driven by an Oscillating Pressure Gradient

CASE OF ONE-DIMENSIONAL FLOW BETWEEN TWO PARALLEL FLAT PLATES

This is the simplest possible example of an internal flow geometry with which to discuss the patterns of fluid flow with changing values of Wo. Consider the one-dimensional flow of a fluid of density ρ and dynamic viscosity μ between two flat parallel plates of length l separated by a distance $2a$ $(2a = L)$, as illustrated in Fig. 1.

The governing equation of motion of the fluid is given by the following form of the Navier–Stokes equation

$$\frac{\partial^2 u(y,t)}{\partial y^2} - \frac{\rho}{\mu}\frac{\partial u(y,t)}{\partial t} = \frac{1}{\mu}\frac{\partial p}{\partial x} \qquad (3)$$

where $u(y,t)$ represents the velocity of the fluid in the x direction, and $\partial p/\partial x$ is the pressure gradient. The boundary conditions follow the standard "no-slip" rule:

$$u(-a,t) = 0, \; u(a,t) = 0 \text{ for all } t. \qquad (4)$$

Consider a pressure gradient $\partial p/\partial x$ which is periodic in time, namely,

$$\frac{\partial p}{\partial x} = \frac{p_2 - p_1}{l} = -Ae^{int} \qquad (5)$$

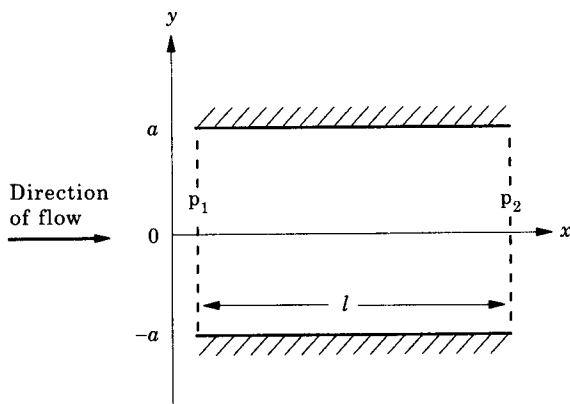where the frequency n was defined above (equation 1),

FIG. 1. One-dimensional fluid flow (in x direction) between two fixed parallel flat plates.

the constant A is real, and i is $\sqrt{-1}$. [Note that $e^{int} = \cos(nt) + i\,\sin(nt)$.]

Although the solution for velocity in this case may be found in the engineering literature (e.g. Landau & Lifshitz, 1959, p. 95; Kurzweg, 1985, p. 292), it is reported in complex form, namely,

$$u(y,t) = \frac{A}{in\,\rho}\left[1 - \frac{\cosh\left(Wo\,i^{1/2}\frac{y}{a}\right)}{\cosh(Wo\,i^{1/2})} \right] e^{int}, \qquad (6)$$

and hence the reader must solve for the real part of this solution (discarding the imaginary components). In order to make the information contained in this mathematical expression more accessible to a broad biological audience, we therefore present the solutions for velocity, total volume flow rate, and the velocity gradient at the wall in explicit (real) form.

The real part of eqn (6) is

$$u(y,t) = \frac{A}{n\rho\gamma}\left\{ [\sinh\Phi_1(y)\sin\Phi_2(y) \right.$$
$$+ \sinh\Phi_2(y)\sin\Phi_1(y)]\cos\,(nt)$$
$$+ [\gamma - \cosh\Phi_1(y)\cos\Phi_2(y)$$
$$\left. - \cosh\Phi_2(y)\cos\Phi_1(y)]\sin(nt)\right\}, \qquad (7)$$

where

$$\Phi_1(y) = \frac{Wo}{\sqrt{2}}\left(1 + \frac{y}{a}\right), \; \Phi_2(y) = \frac{Wo}{\sqrt{2}}\left(1 - \frac{y}{a}\right), \qquad (8)$$

$$\gamma = \cosh(\sqrt{2}Wo) + \cos(\sqrt{2}Wo).$$

The amplitude of this oscillating velocity, u_{max}, is:

$$u_{max} =$$
$$\frac{A}{n\rho\gamma}\left\{ [\sinh\Phi_1(y)\sin\Phi_2(y) + \sinh\Phi_2(y)\sin\Phi_1(y)]^2 \right.$$
$$+ [\gamma - \cosh\Phi_1(y)\cos\Phi_2(y)$$
$$\left. - \cosh\Phi_2(y)\cos\Phi_1(y)]^2\right\}^{0.5} \qquad (9)$$

The volume flow rate of the fluid through a unit depth, $Q(t)$, is given by

$$Q(t) = \int_{-a}^{a} u(y,t)\,dy \qquad (10)$$

or

$$Q = \frac{2Aa^3}{\mu} \left\{ \frac{(\Theta_1 - \Theta_2)}{\sqrt{2Wo^3}} \cos(nt) \right.$$

$$\left. - \frac{(\Theta_1 + \Theta_2) - \sqrt{2Wo}}{\sqrt{2Wo^3}} \sin(nt) \right\}, \qquad (11)$$

where

$$\Theta_1 = \frac{\sinh(\sqrt{2}Wo)}{\gamma}, \ \Theta_2 = \frac{\sin(\sqrt{2}Wo)}{\gamma}. \qquad (12)$$

The amplitude of this oscillating volume flow rate, Q_{max}, is

$$Q_{max} = \frac{2Aa^3}{\mu \ Wo^3} \sqrt{\left(\frac{\sinh(\sqrt{2}Wo)}{\gamma}\right)^2 + \left(\frac{\sin(\sqrt{2}\ Wo)}{\gamma}\right)^2 - \frac{\sqrt{2}Wo[\sinh(\sqrt{2}Wo) + \sin(\sqrt{2}Wo)]}{\gamma} + Wo^2} \qquad (13)$$

The velocity gradient at the wall is

$$\frac{du(a,t)}{dy} = \frac{-A \ Wo}{\sqrt{2} \ n \ \rho a \ \gamma}$$

$$\left\{ [\sinh(\sqrt{2}Wo) + \sin(\sqrt{2}Wo)]\cos \ (nt) \right.$$

$$\left. + [\sinh(\sqrt{2}Wo) - \sin(\sqrt{2}Wo)]\sin(nt) \right\}$$

$$\qquad (14)$$

$$= -\frac{du(-a,t)}{dy}$$

The maximum velocity gradient [the amplitude of eqn (14)], $(du(a,t)/dy)_{max}$, is

$$\left(\frac{du(a,t)}{dy}\right)_{max}$$

$$= \frac{A \ Wo}{n \ \rho a \ \gamma} \sqrt{[\sinh(\sqrt{2}Wo)]^2 + [\sin(\sqrt{2}Wo)]^2} \qquad (15)$$

CASE OF ONE-DIMENSIONAL FLOW INSIDE A CIRCULAR CYLINDER

As already noted, a mathematical expression allowing the prediction of velocity profiles for the case of flow inside a circular cylinder subjected to a longitudinal oscillating pressure gradient may be found in Womersley (1955). Because that equation contains Bessel functions, Womersley supplied tables

to aid in the numerical approximation of velocity at any point in time. It is worth noting that mathematically less complex expressions for the same geometry (written as series approximations) appear in White (1991; pp. 135–136). Because the relationship of velocity to the other parameters changes so drastically with Wo, White supplied different equations for the two cases of $Wo < 2$ and $Wo > 2$ (note that White used a different notation: White's $\omega^* = Wo^2$).

Fluid Behavior Predicted from the Magnitude of Wo

The equations supplied above for the case of flow between parallel flat plates predict fluid behavior which is qualitatively similar to that seen in the case of flow inside a cylinder. Therefore, although the graphs below will specifically correspond to the case of flow between parallel flat plates, the two cases will be discussed together, with quantitative differences identified when appropriate. This allows generalizations to be made for flow inside biological structures for the range of geometries that encompass these two cases (subject to the assumptions discussed below).

VELOCITY PROFILES

A generalization that may be made for any spatial location within an enclosed fluid subjected to an oscillating pressure gradient as defined above (e.g. the fluid is confined to one-dimensional motion) is that the velocity at that point will vary sinusoidally with the same frequency as the driving pressure gradient (for a given Wo). This becomes clear from examination of eqn (7) above [or the series approximations in White (1991) for the cylindrical case]. Note that for any given Wo (i.e. a given frequency, gap size, and fluid viscosity) and y (position relative to a wall), eqn (7) is simply a cosine term added to a sine term of the same frequency but different amplitude; i.e., eqn (7) reduces to $u(t) = c_1\cos(nt) + c_2\sin(nt)$ which in turn can be simplified as $u(t) = c_3\cos(nt - \phi)$ where $c_3 = \sqrt{c_1^2 + c_2^2}$ [for useful discussion of trigonometric properties see Caro et al. (1978, pp. 106–129)]. These velocity oscillations may be out of phase with the driving pressure gradient and the amplitude of the velocity oscillations may be affected; the magnitude of Wo will determine both the degree of this phase shift

Time course of pressure gradient causing flow:

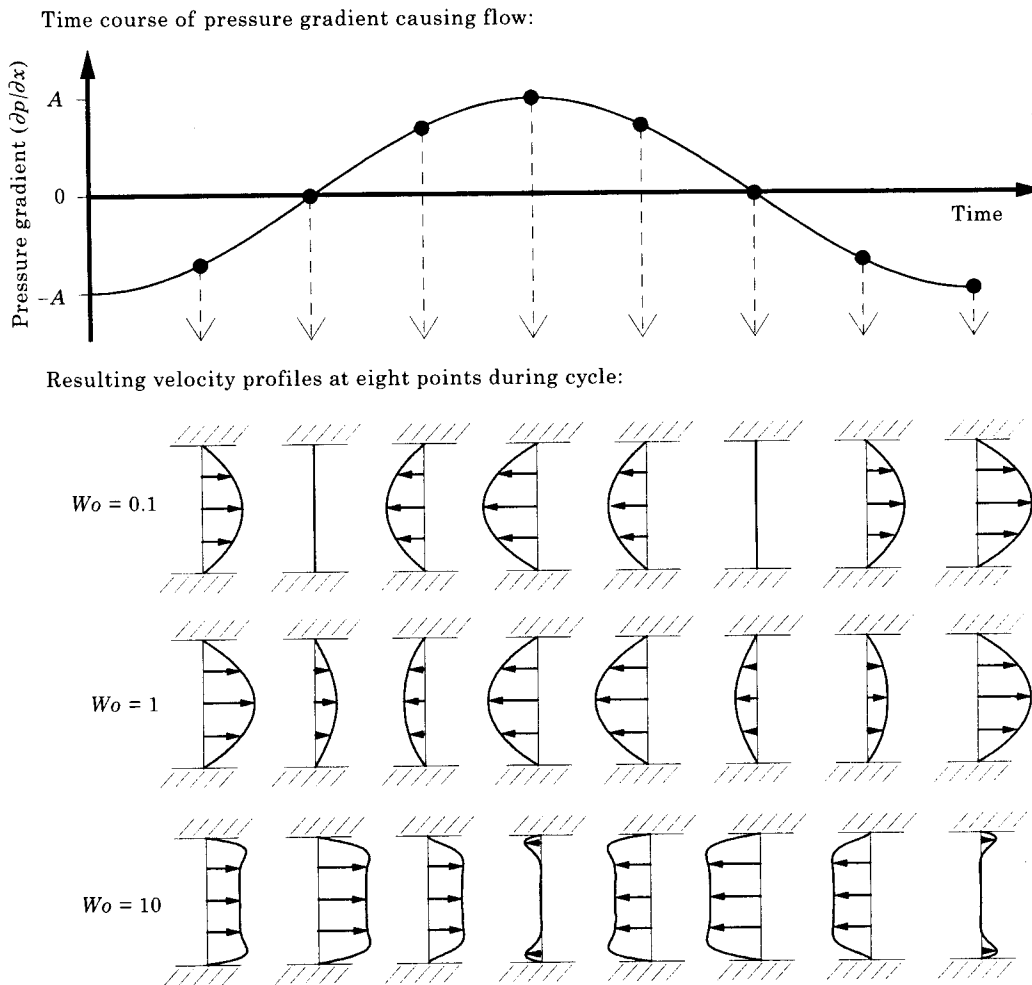Resulting velocity profiles at eight points during cycle:

FIG. 2. Velocity profiles between two flat plates at eight points in time during a single cycle of a sinusoidally-varying pressure gradient for three values of the dimensionless Womersley number. The length of a horizontal arrow indicates the magnitude of the velocity for that location and is non-dimensionalized by dividing by the maximum velocity at any location during a complete cycle. A is assumed to be a positive constant.

and the change in amplitude relative to the steady state case.

The effect of Wo on this behavior of the fluid can most easily be visualized by examining velocity flow profiles. Examples of velocity profiles for different values of Wo at eight different points in time during a single cycle of an oscillating pressure gradient (Fig. 2) show many characteristics shared by fluid behavior inside circular cylinders (Caro et al., 1978). When $Wo < 1$, the fluid behaves in a quasi-steady manner: the velocity profile corresponds closely to that expected for the instantaneous value of the pressure gradient driving the flow ($\partial p/\partial x$). For example, when the pressure gradient is zero ($\partial p/\partial x = 0$), the velocity of the fluid is negligible at every point across the gap. When $Wo = 1$, the velocity flow profiles still exhibit the rounded Poiseuille shape but they begin to show a phase lag with respect to the pressure gradient; e.g.

when the pressure gradient is zero there is still perceptible flow in the decelerating fluid (Fig. 2). As Wo increases further (e.g., $Wo = 10$, Fig. 2), the phase lag becomes much more pronounced and the velocity profiles change shape; the maximum velocity is no longer centered between the two plates.

Another change in the flow that occurs with an increase in Wo is a change in the amplitude of the velocity oscillations; this cannot be seen in Fig. 2 because the velocity profiles were drawn to different scales for different Wo values to make differences in their shapes visible. The amplitude of the velocity oscillations will show the same basic pattern for all spatial locations; Fig. 3 shows the predictions at the midplane ($y = 0$). It is usual to present graphs such as this in dimensionless form to present as general a conclusion as possible. In Fig. 3 the velocity at the midplane ($u(0,t)$) is normalized relative to u_{steady}, the

maximum steady velocity that would result if the driving pressure gradient was held constant at its minimum (i.e. greatest negative) value:

$$\frac{\partial p}{\partial x} = -A; \quad u_{steady,\, y = 0} = \frac{Aa^2}{2\mu} \qquad (16)$$

[eqn (16) may be found in any introductory fluid mechanics textbook such as Fox & McDonald (1978)].

Figure 3(a) shows a single oscillation of the pressure gradient. In Fig. 3(b) the resulting velocity oscillations are depicted for the corresponding points in time during this single cycle (time is normalized by the length of the period). Thus, Fig. 3 illustrates that for low Wo ($Wo < 1$), the amplitude of the oscillating velocity is approximately equal to u_{steady}. However, as Wo exceeds 1 in magnitude, the amplitude of the oscillating velocity quickly declines relative to the steady-state case.

While the dimensionless presentation seen in Fig. 3 is very useful, it does obscure an important feature of the fluid behavior that is more obvious when velocity is graphed without normalizing relative to the steady-state standard. This feature is that the (non-normalized) velocity oscillations will either increase *or* diminish in amplitude depending on whether the change in Wo is caused by a change in size (a) or frequency (n) (Fig. 4). This fact is not obvious from Fig. 3 simply because $u(y,t)$ scales differently than u_{steady} with a and n [comparing eqn (7)
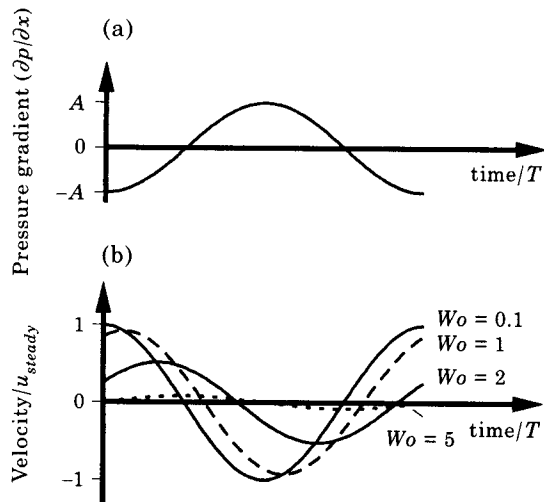

FIG. 3. (a) Sinusoidally-varying pressure gradient driving flow between flat plates (A is assumed to be a positive constant). (b) The resulting sinusoidally-varying velocity undergoes both a phase shift and an amplitude change as Wo increases. The velocity at midplane ($y = 0$) is shown for four values of Wo, and is normalized by dividing by the steady-state velocity defined in the text. A single cycle covers the same distance on the x-axis when the time is normalized by dividing by T, the period (the length of time of 1 cycle).
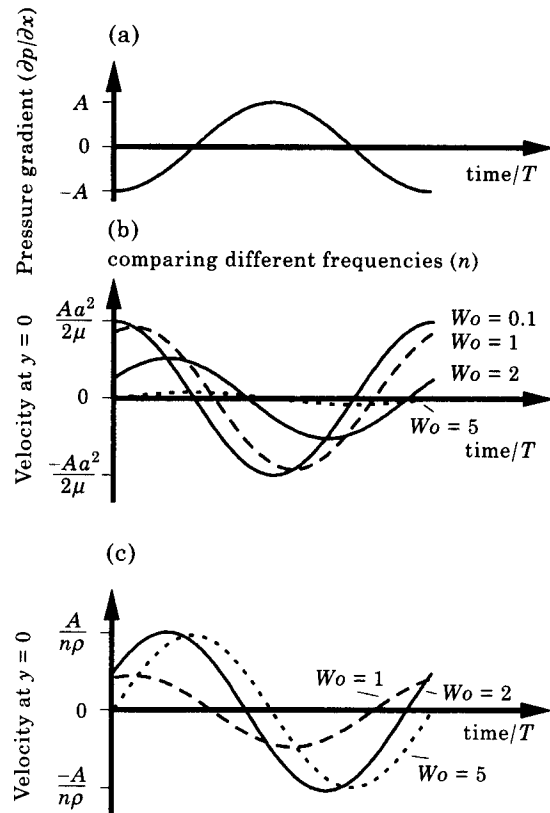

FIG. 4. (a) Sinusoidally-varing pressure gradient driving flow between flat plates (A is assumed to be a positive constant). Same as Fig. 3(a). (b) and (c) The resulting sinusoidally-varying velocity undergoes both a phase shift and an amplitude change as Wo increases. The velocity halfway between the plates ($y = 0$) is shown, but unlike Fig. 3 is not normalized relative to a standard. (b) Wo increases by increasing n, holding a constant. The amplitude of the velocity oscillations diminishes with increasing Wo. (c) Wo increases by increasing a, holding n constant. The amplitude of the velocity oscillations increases with increasing Wo until $Wo \approx 3$. The velocity oscillations corresponding to $Wo = 0.1$ are not graphed because they are not perceptibly different from the line marking the x-axis.

with eqn (16) noting that $A/n\rho$ may be written as $Aa^2/Wo^2\mu$].

In Fig. 4, graphs (b) and (c) contrast the flow response to increasing Wo depending on whether the pressure gradient is oscillating more frequently [graph (b), n is changing] or if the surfaces are farther apart [graph (c), a is changing]. When the frequency is sufficiently high that Wo exceeds one in magnitude, the amplitude of the velocity oscillations decreases precipitously relative to that seen at lower frequencies [Fig. 4(b)], as if the fluid cannot "keep up" with the rapid reversals in pressure gradient (especially fluid located farther from the walls). In contrast, when Wo increases due to a larger gap size, the velocity oscillations increase in amplitude (bottom graph) until Wo exceeds some critical value. The magnitude
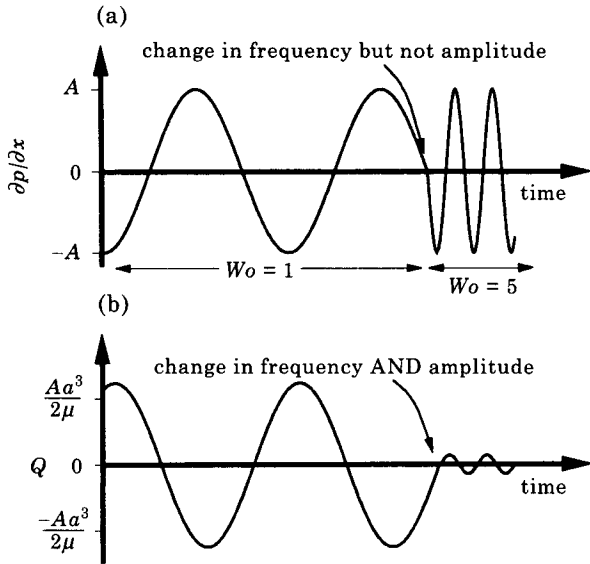
FIG. 5. (a) The sinusoidally-varying pressure gradient increases in frequency (corresponding to an increase in Wo from 1 to 5) but not amplitude. (b) The corresponding change in the volume flow rate between the two flat plates shows a change in both frequency and amplitude. A is assumed to be a positive constant.

of this critical value changes with location (y), and is approximately three for this example ($y = 0$). Notice that in either case (changing n or a), as Wo increases, the velocity oscillations become more and more out of phase with the oscillating pressure gradient.

VOLUME FLOW RATE

For some physiological functions, the total flow rate through a gap or tube is of greater interest than the velocity profile. Not surprisingly, volume flow rate varies with Wo in a virtually identical manner to the variation already described for the velocity measured at any point; i.e., if the driving pressure gradient oscillates more rapidly without changing amplitude,

the corresponding oscillations in total flow also increase in frequency but decrease in amplitude when the frequency is high enough such that $Wo > 1$. A simple graphical example of what is meant by this may be seen in Fig. 5.

A graph showing the general pattern of the decrease in amplitude of the oscillating volume flow rate with increasing Wo is shown in Fig. 6 for values of $0 < Wo \leq 10$ for the case of flow between parallel flat plates. This graph is virtually identical to the original illustration in Womersley (1955) for the case of flow inside a cylinder; identical definitions were used to facilitate comparisons. The amplitude of the oscillating volume flow rate, Q_{max} [eqn (13)], is normalized by dividing by the magnitude of the maximum steady flow that would result from the steady application of the minimum pressure gradient (Q_{steady}, defined graphically in Fig. 6). Q_{steady} for the case of flat plates is

$$Q_{steady} = \frac{2Aa^3}{3\mu} \tag{17}$$

Note that the amplitude of the oscillating volume flow rate drops sharply for values of $Wo > 1$ (Fig. 6); at $Wo = 1$ the amplitude is 92% of its steady-state value, while the amplitude is halved by $Wo = 2$. This drop is even sharper than that seen for the geometry of flow inside a circular cylinder, where the amplitude is not halved until $Wo > 3$ (see fig. 2; Womersley, 1955). As seen in the velocity relationships above, use of the (standard) normalizing process obscures the differences in flow expected if a change in Wo results from a change in frequency or size. A decrease in the amplitude of the (non-normalized) oscillating volume flow rate as depicted in Fig. 6 would be expected only for the case of increasing frequency. For the case of Wo increasing only with size (such as identical oscillating pressure gradients reaching gaps that differ
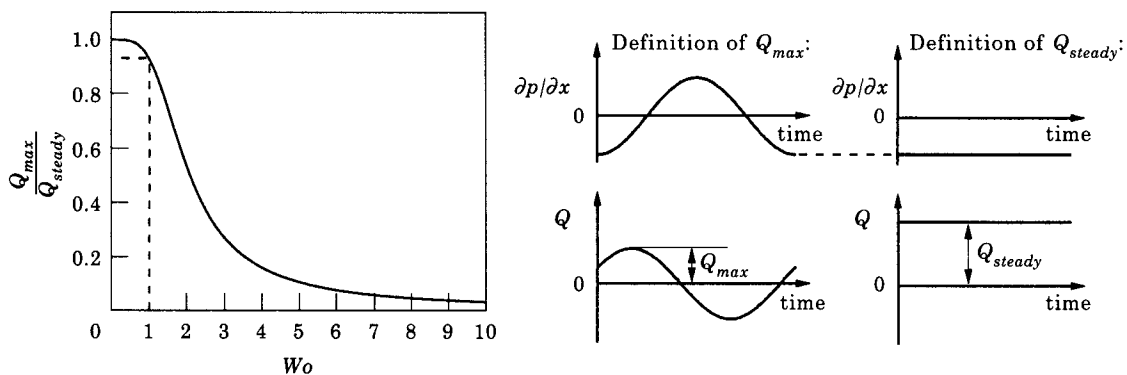

FIG. 6. As Wo increases, the maximum volume flow rate, Q_{max} (the amplitude of the sinusoidally-varying Q), is a smaller and smaller fraction of the corresponding steady-state value Q_{steady} (the volume flow rate that would result from a constant pressure gradient of the magnitude of the amplitude of the varying pressure gradient).
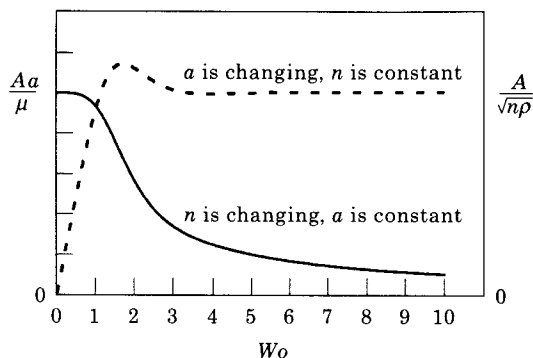
FIG. 7. The magnitude of the maximum velocity gradient at the wall ($|du/dy|_{max}$ at $y = a$ or $y = -a$) during oscillatory flow changes dramatically with a change in Wo when $Wo = O(1)$. Whether $|du/dy|_{max}$ increases or decreases with increasing Wo depends on whether the increase in Wo is caused by an increase in gap width (dashed line) or an increase in oscillation frequency (solid line). A is assumed to be a positive constant.

in size), the amplitude of the oscillating volume flow rate would be expected to increase monotonically with size in the range $0 < Wo \leq 10$.

VELOCITY GRADIENT AT THE WALL

What does this oscillating flow "feel" like at the wall? The shear stress at an infinitesimal area of wall is directly proportional to the local velocity gradient (du/dy at $y = a$ or $y = -a$), so therefore a changing velocity profile will lead to a changing shear stress at the wall. It follows from eqn (14) that the stress on the wall will also vary sinusoidally with time at the same frequency as the oscillating pressure gradient. The magnitude of the maximum force on the wall during a cycle will depend on Wo, n, and a [eqn (15)]. For an increase in oscillation frequency that causes Wo to exceed one in magnitude, there is a rapid decrease in the maximum velocity gradient at the wall (Fig. 7) despite the change in the shape of the velocity profile (Fig. 2). This decline (Fig. 7) is very similar to the decline seen in the volume flow rate (Fig. 6); in both cases, the amplitude has dropped to about 92% of its maximal (steady) value at $Wo = 1$, and is halved close to $Wo = 2$. The main difference can be seen for the higher Wo's, where the amplitude has dropped to only 10% of its maximal value at $Wo = 10$ for the velocity gradient (Fig. 7), but the amplitude of the volume flow rate had dropped to 10% of its maximal value by $Wo = 5$ (Fig. 6). This difference in rate of decline is a direct consequence of the change in shape of the velocity profile with higher Wo (Fig. 2); the fluid oscillating nearer the walls at higher Wo affects the wall shear stress more substantially than it contributes to the total volume flow oscillations. For an increase in gap width (Fig. 7, dashed line), the

maximum force on the wall will increase dramatically when the value of Wo lies within the range $0 < Wo < 2$ but will be relatively insensitive to further increases in gap width that cause Wo to exceed about three in magnitude.

Discussion

Unsteady flow, common in biological systems (Vogel, 1994a), can greatly complicate efforts to make even a qualitative description of physiological processes that are affected by flow. Therefore, the identification of simple guides to unsteady fluid behavior is very useful. Guides to mechanical behavior often take the form of dimensionless numbers, which are groupings of parameters that define the system geometry and physical properties such that all units cancel (McMahon & Bonner, 1983; Pennycuick, 1992). The magnitude of a dimensionless number can usually be related to the relative importance of competing mechanical phenomena for a specific set of circumstances, thereby allowing insight into some mechanical events, such as whether a fluid is likely to exhibit laminar or turbulent behavior, for example.

Along these lines, one interpretation of the Womersley number is the ratio of the characteristic depth measured within the fluid ($L/2$) to the depth of the oscillating boundary layer, which will be on the order of $\sqrt{(v/n)}$ for a variety of geometries in unsteady flow [e.g. inside cylinder, (Pedley et al., 1977), rotating disk, oscillating flat plate (Schlichting, 1979)]. (The relevance of $L/2$ instead of L for comparison with the depth of the boundary layer is most obvious for cases of internal flow, where a lumen diameter includes two boundary layers.) Thus, when $Wo < 1$, the oscillating boundary layer straddles the entire fluid gap or space, while for $Wo > 1$, the oscillating boundary layer is confined close to the surface (e.g. see velocity profiles in Fig. 2). Note that this is an order-of-magnitude physical description and should not be applied as an exact solution for any arbitrary geometry. Despite this caveat, it should be obvious that there is no physical reason to limit the application of Wo to internal one-dimensional oscillating flow, and many of the inferences drawn in this paper will be approximately valid for many other situations. We will return to this point after discussing the implications of the analysis for one-dimensional internal flow.

It was shown in the above analysis that an unsteady flow through a gap between two parallel flat plates qualitatively follows the same behavior demonstrated earlier for longitudinal flow inside a circular cylinder

(Womersley, 1955). Specifically, the magnitude of the same dimensionless group, Wo [eqn (1)], can be used to predict the unsteadiness of flow responding to an oscillating pressure gradient, with the flow faithfully tracking the time-varying pressure gradient when $Wo < 1$ ("quasi-steady") and becoming less responsive to changes when $Wo > 1$. In addition, a phase shift is expected between the pressure gradient and the flow when $Wo > 1$. Therefore, flow through any gap, opening, or passage that falls within the range of these geometries may be characterized in its time-dependent response in part by the magnitude of Wo; the more closely the biological geometry comes to these mathematical ideals, the more closely the quantitative fit of the predictions of flow behavior (also subject to the assumptions in the analysis; see below for discussion).

While the magnitude of Wo by itself will allow the insights into the fluid behavior just stated above, there are additional aspects to the fluid behavior that are not obvious in a completely non-dimensional formulation. That is, a change in size will have a completely different effect on the (absolute) oscillation amplitude of the flow than a change in frequency even if identical values of Wo are generated. This is true whether flow is described by velocity, the volume flow rate, or the velocity gradient at the surface (all discussed explicitly above). For example, if Wo increases due to an increase in the frequency of the driving pressure gradient (in the absence of other changes), the amplitudes of the unsteady component of the flow are expected to decrease sharply for velocity, volume flow rate, and the velocity gradient at the surface, when the magnitude of Wo exceeds one. That is, the flow will seem much less unsteady as it passes through the gap. On the other hand, if the oscillating pressure gradient remains constant and the size of the gap through which the fluid can move is increased, the velocity and velocity gradient oscillations will become amplified (the amplitudes of the unsteady components will increase) but only up to a value of $Wo \approx 2$. For $Wo > 2$, further increases in size will not be reflected in significant increases in amplitude for the velocity and velocity gradient oscillations (e.g. see Figs 3 and 6). The volume flow rate oscillations will continue to increase with Wo as long as the assumptions of the analysis are valid. Note that the amplitude of the driving pressure gradient has been held arbitrarily constant (A) in this discussion. If A has some relationship with another variable (such as A increasing with frequency) then the flow may become either more or less unsteady (in amplitude) with a change in Wo

depending not only on the magnitude of Wo but also on this relationship.

What are the biological ramifications of this pronounced change in fluid behavior as the magnitude of Wo crosses the critical value of one? Clearly, a given structure may function in a different manner when exposed to different frequencies of oscillating pressure gradients, experiencing pronounced unsteady flow through gaps at lower frequencies and almost no unsteady flow at higher frequencies. In fact, this analysis shows that there is an upper frequency limit for maintaining significant tidal flow through a gap of a given size, corresponding to the frequency at which $Wo \approx 1$.

EXAMPLES OF OSCILLATING INTERNAL FLOW IN BIOLOGICAL SYSTEMS

The case of internal flow within cylinders in the biological context of blood circulation has a tremendous literature and is described as the most advanced branch of biomechanics (Fung, 1997, p. v). Because flow inside cylinders has been so thoroughly discussed in the biological literature, it will not be discussed further here (e.g. see Caro et al., 1978; Fung, 1997). Instead, other examples of oscillating internal flow will be very briefly noted; both for another geometry (flow between flat plates) and other physiological functions (e.g. sensory systems).

What range of Womersley numbers exist for unsteady internal flow in biological systems? Wo is a function of size, frequency, and kinematic viscosity of the fluid [eqn (1)]. Therefore, for a given fluid (with a given kinematic viscosity), the range of combinations of frequencies and sizes for which $Wo < 1$ and $Wo > 1$ can be identified (Fig. 8). For example,
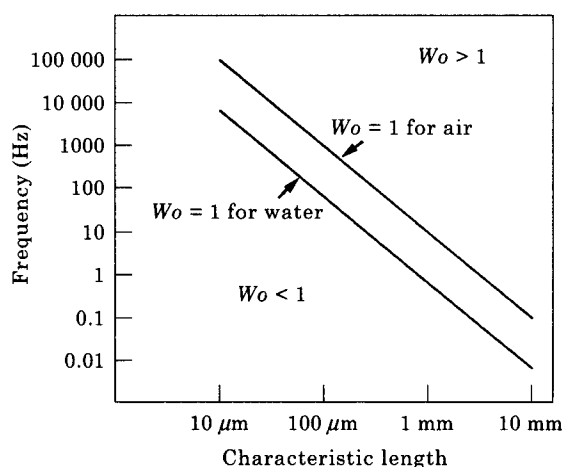

FIG. 8. The combinations of frequency and size (gap) for which $Wo < 1$, $Wo = 1$, and $Wo > 1$ are identified for two examples of fluids (air, $v = 15 \times 10^{-6}\,m^2\,s^{-1}$; water, $v = 1 \times 10^{-6}\,m^2\,s^{-1}$).

(a)

(b)

1 mm

1 mm

(c)

(d)

(e)

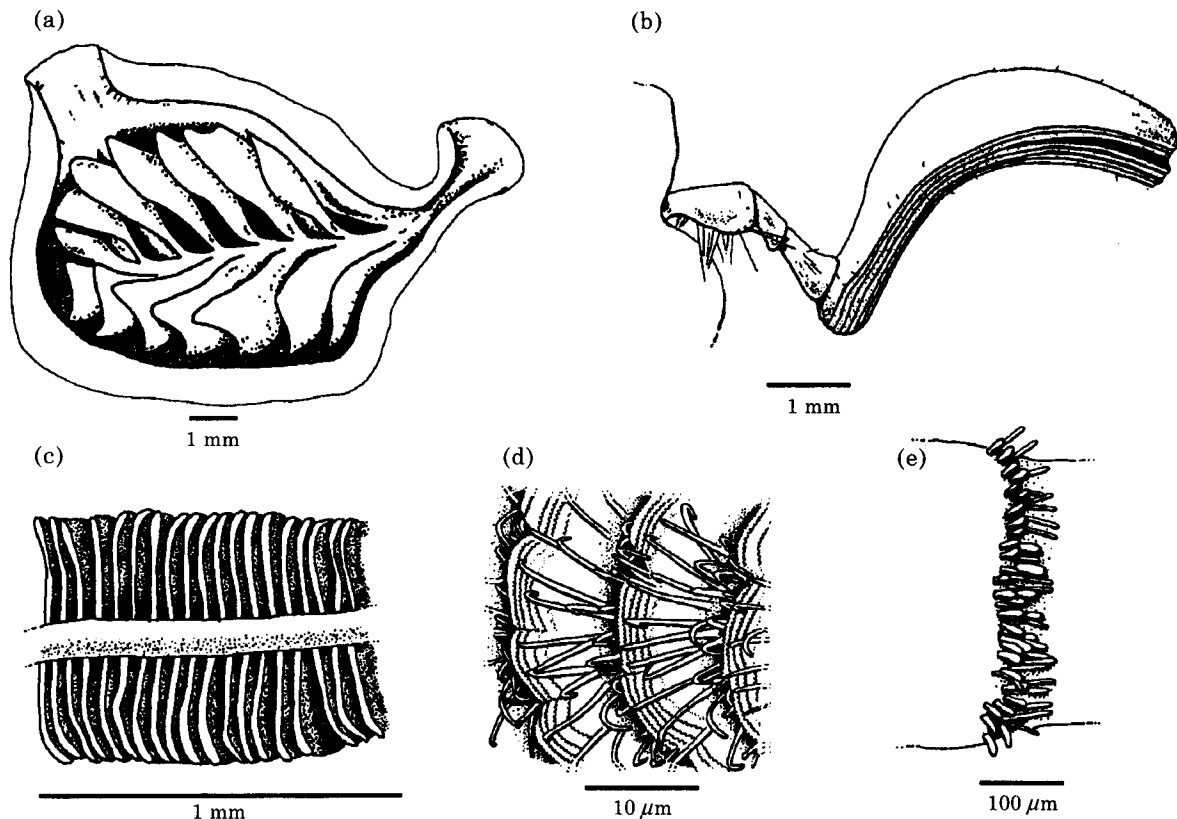1 mm   10 μm   100 μm

FIG. 9. Examples of flat plates in biological systems. (a) Fish olfactory organ with wall of chamber removed, viewed from side [redrawn with permission from Kleerekoper (1969, *Olfaction in Fishes*. Bloomington: Indiana University Press, figure 27, p. 51), *Anguilla anguilla*, scale estimated from other sources]. Water flows from the anterior naris (seen at right) to posterior naris (left) passing between the lamellae. (b) Beetle antenna viewed from dorsal vantage (redrawn from unpublished scanning electron micrograph by R. J. Elzinga, *Polyphylla* sp.). Air passes between the seven lamellae (shown in closed position). (c) Fish gill viewed from the buccal chamber [redrawn with permission from Ellis & Smith (1983, *J. Exp. Zool.* **227**, 371–380, figure 2), *Anguilla anguilla*). Water passes between lamellae into the plane of the figure. (d) Surface of moth antenna viewed in high magnification illustrating the location of sensory hairs between flat scales [redrawn with permission from Van Der Pers *et al.* (1980, *Int. J. Insect Morphol. Embryol.*, **9**, 15–23, figure 2), *Yponomeuta malinellus*]. Distal is to the right. (e) Surface of stonefly antenna illustrating linear array of cylindrical sensory hairs [redrawn with permission from Kapoor (1985, *Int. Insect Morphol. Embryol.*, **14**, 273–280, figure 2C), *Paragnetina media*]. Distal is to the right.

air passing through any gap or opening less than 1 mm in size will show quasi-steady behavior ($Wo < 1$) if exposed to a driving pressure gradient frequency of 10 Hz or less. For frequencies of 1 Hz or less, $Wo < 1$ for gaps ≤ 5 mm. Because water is 15 times less kinematically viscous than air [for general discussion see Denny (1993); and Vogel (1994a)], water oscillating at one-fifteenth of the same frequency as air oscillating through a gap of the same size will lead to flow with the same magnitude of Wo [eqn (1); Fig. 8]. On the other hand, because of the squareroot term, the same oscillation frequency through the same gap size will lead to a Wo approximately four times greater ($\sqrt{15}$) in water than in air. This latter point is particularly significant when considering mechanoreception in water vs. air.

Surfaces shaped approximately like parallel flat plates do occur in biological systems, especially for surfaces involved in exchange processes (Vogel 1994a, p. 300) (Fig. 9). For example, in fish, both gills and olfactory organs are commonly composed of parallel flat surfaces between which water flows (Hughes, 1966, 1984; Kleerekoper, 1969; Hara, 1975) [Fig. 9(a) and (c)]. As another example, while individual sensory hairs on arthropods are often cylindrical in shape (Ghiradella *et al.*, 1968; Altner & Prillinger, 1980), they may be laterally flattened and thus more plate-like (Olson & Andow, 1993), located on flat surfaces arranged in parallel arrays [Fig. 9(b) and (d); Inouchi *et al.*, 1987], or arranged in linear arrays perhaps better approximated as flat plates than as single isolated cylinders [Fig. 9(e); Payne *et al.*, 1973, Van Der Pers *et al.*, 1980, Gleeson *et al.*, 1993]. In some cases, such as these externally-projecting sensory structures, the relevant flow is difficult to characterize as either strictly external or internal flow

and will have attributes of each. These biological flat surfaces may experience unsteady flow either because of the behavior of an associated pump or because of the unsteady nature of the ambient fluid due to a mechanical disturbance.

From consideration of Fig. 8, it seems probable that many of the flows driven by biological pumps between flat plate-like exchange surfaces will have $Wo \leq 1$, due to the combination of small gap sizes and relatively low frequencies. For example, consider fish gills, that have been the subject of detailed examination. Water flow between lamellae in fish gills is usually unsteady because the water flow is driven by muscular pumping; these muscular pumps occur on both the "upstream" (buccal) and "downstream" (opercular) sides of the gill (sometimes visualized in figures as two pistons driving an oscillating pressure gradient, e.g. Hughes, 1984). Steady-state (Hagen–Poiseuille) equations are usually used as a first approximation during analysis of gas exchange in fish gills even for fish with pulsatile water movement across their gills (e.g. Hughes, 1984; Piiper & Scheid, 1984). Wo is probably less than one in magnitude in this case: e.g. an estimate of $Wo \leq 0.2$ results from a distance between lamellae in a fish gill ≈ 20–100 µm (Piiper & Scheid, 1984), frequency of pulsatile water flow ≈ 0.5–1 Hz (Holeton & Jones, 1975), and kinematic viscosity of seawater $\approx 1 \times 10^{-6}$ m^2 s^{-1} (at 20°C, Vogel, 1994a). Naturally any additional factors such as lamellar movements [unknown but identified as a possible complication by Randall & Daxboeck (1984)] would greatly influence the flow conditions.

Unlike biological pumps (at least the so-called positive-displacement pumps; Vogel, 1994b), which often operate in the frequency range on the order of 1 Hz, oscillations in the ambient fluid commonly have frequencies on the order of 10 or 100 Hz (such as the "near-field" component of sound or disturbances set up by oscillating appendages). Therefore, flow through sensory structures detecting oscillations in fluid could experience $Wo > 1$. Recall that for $Wo > 1$, most of the oscillating fluid flow is near the surface. Thus, Denton & Gray (1989) point out that for the fish lateral-line system (a peripherally-located mechanosensory organ used in schooling behavior, obstacle avoidance, and detection of prey), a wide range of Wo's are found corresponding to the wide range of frequencies for which lateral lines are thought to operate (Denton & Gray refer to "Wo" as "k"). Because the larger canals (1 mm in internal diameter) will operate in $Wo > 1$, the changing velocity profile will be confined to the sides of the canal even for low frequencies of a few Hz; they

suggest that this explains why very short sensory units ("cupulae") are sometimes found in the very large canals.

It is not just mechanosensory systems that deal with fluid of an oscillatory nature; it has been noted repeatedly that air or water flow is frequently unsteady as it approaches a chemoreceptive surface on an organism (Schmitt & Ache, 1979; Atema, 1985; Dusenbery, 1992). For example, in the presence of appropriate chemical stimuli, mammals sniff, fish sniff, reptiles flick their tongues, crustaceans flick their antennules (which are covered with sensory hairs) and fan their thoracic appendages, and insects wave their antennae (covered with sensory hairs) and fan their wings (these fanning behaviors exhibited by arthropods will change the air flow over chemosensory structures among other possible functions) (Schneider, 1964; Macrides & Chorover, 1972; Nevitt, 1991; Gleeson et al., 1993; Cooper, 1994; Schwenk 1994). Although the term "sniffing" is used whether unsteady fluid is moved across a chemosensory surface or whether the chemosensory organ is oscillated through a fluid, the formulation in this paper is most appropriately applied to the former class of cases (primarily because of amplitude differences). Differences between these two cases will be the subject of a future communication.

What is the magnitude of Wo for cases of an oscillating flow applied to an olfactory structure that may be approximated as an array of gaps? A necessarily rough estimate of available frequencies and gap sizes suggests that for sniffing in vertebrates (frequency on the order of 1 Hz, gaps often <1 mm across) and wing-fanning in insects (frequency on the order of 50 Hz, gaps between flat surfaces on antennae often <100 µm), Wo's will often be below 1 in magnitude (see Fig. 8). In these cases, quasi-steady conditions will exist for air or water passing across the olfactory receptors. This means that the flow will vary in phase with the unsteady flow of air or water supplied to the chemoreceptive surfaces and will not exhibit the lower amplitudes associated with higher values of Wo. Note that this does not necessarily imply perception of an unsteady interception of chemical signal molecules, because the perception of signal interception will depend on the temporal characteristics of the sensory neurons as well (Atema, 1987, 1988; Christensen & Hildebrand, 1988). Whether this low Wo flow profile, that results in the bulk of the fluid being maximally distant from the intercepting surfaces, is a significant barrier in terms of the diffusion of the signal molecules to the receptive surfaces will depend on the magnitude of the diffusion coefficient(s) of the signal molecule(s) of

interest (Murray, 1977; DeSimone, 1981; Hahn et al., 1994; Koehl, 1996). The dimensionless number that quantifies the diffusion coefficient relative to the physical properties of the surrounding fluid is the Schmidt number (Sc = kinematic viscosity/diffusion coefficient), although there are additional dimensionless numbers useful in describing mass transport.

ASSUMPTIONS OF ANALYSIS

A primary assumption of the mathematical analysis is that the flow is one-dimensional. This means that while the physical setting may be three-dimensional, velocity will vary only with distance from the wall ($u(y,t)$ not $u(x,y,z,t)$). This will be approximately true for flow in a gap or tube in the absence of turbulence. Turbulence is the macroscopic mixing between adjacent fluid layers, in contrast to the laminar behavior seen in slower flows in which the fluid layers slip smoothly past each other. The flow behavior (laminar or turbulent) for a steady-state situation is determined by the value of the Reynolds number [eqn (2)]. For steady flow inside a cylinder or between parallel walls this transition from laminar to turbulent flow takes place at speeds corresponding to $Re \approx 2000$ [flat plates, $Re \approx 1400$; circular cylinder $Re \approx 2300$; Fox & McDonald (1978); Re is calculated from eqn (2) using the average cross-sectional velocity for U_0 and the distance between the plates or the diameter of the cylinder for L]. These transition Re's are approximate because in practice they also depend on other factors such as the roughness of the surface (Fox & McDonald, 1978; Vogel, 1994a).

For oscillating flow, where u is changing, Re based on instantaneous velocity (averaged over the flow cross-section) will also be changing. It follows that during oscillating flows that span the transition Re, the flow might become periodically turbulent when the flow is at its fastest and then return to laminar behavior during the slower flow parts of the cycle, and this is in fact what is observed (Nerem & Seed, 1972; Merkli & Thomann, 1975; Kurzweg et al., 1989; Choi & Wroblewski, 1993). However, the transition Re's for oscillating flow may differ from the transition Re's for steady state flow. It has been found empirically that the transition between laminar and turbulent flow in oscillating flow is affected by the magnitudes of both Re and Wo especially when $Wo > 8$; for measurements within glass tubes the transition Re's were approximately 700 times the magnitude of Wo for $Wo > 8$ (Kurzweg et al., 1989; non-invasive flow measurement; Wo range 5–20; Re_{max} range 1500–20 000) while for measurements within a dog's blood vessel the transition Re's were 150–250 times the

magnitude of Wo (Nerem & Seed, 1972; hot-film probe; Wo range 5–30; Re_{max} range 1000–8000). Therefore, the assumption of laminar flow is probably valid for $Re_{max} < 5000$ and $Wo < 20$ for the geometries under question.

It also follows from the assumption of one-dimensional flow that velocity is independent of downstream location. Thus, the analysis herein will be most applicable to the middle of longer channels (avoiding "edge" effects) and especially for lower Re flow where those edge effects are less extensive (Fox & McDonald, 1978; Vogel, 1994a). Because the entrance length for oscillating flow is inversely proportional to the frequency of oscillation (Caro et al. 1978; p. 321), edge effects will also be less extensive at higher Wo. The mathematical assumption of independence of downstream location also means that length-dependent acoustic phenomena such as resonance, or propagation of the "far field" aspects of sound are not described by these mathematics [for useful discussion on this latter topic see Camhi (1984); Dusenbery (1992) and Fletcher (1992)]. However, the "near field" or "displacement component" of sound, which describes the bulk oscillation of the medium, does correspond to this formulation.

ADDITIVE NATURE OF STEADY AND UNSTEADY FLOW COMPONENTS

All of the preceeding discussion and analysis has assumed a pressure gradient with a zero average that results in zero net flow; i.e., the pressure gradient alternates between positive and equivalent negative values, driving an oscillating fluid volume that goes nowhere on average. For many of the biologically important unsteady flows, the average pressure gradient and the average flow are not zero, and so the relevance of the preceeding analysis for cases with non-zero net flow must be questioned. Curiously, this point often receives only brief mention if any; in the original analysis (Womersley, 1955), the mathematical treatment explicitly assumed an average net pressure gradient of zero with no net flow, although a statement was made that a steady flow term was not included. Clearly blood does experience net flow in one direction through the body; McDonald (1955) noted this and suggested that the steady flow component may be simply added to the unsteady oscillating component(s), although his suggestion was made in the absence of mathematical proof or reference.

Addition of steady and unsteady solutions means that if the driving pressure gradient $\partial p / \partial x$ is a combination of an oscillatory ($-Ae^{int}$) and a constant

component $(-P_0)$, then the corresponding velocity $u(y,t)$ must satisfy

$$\frac{\partial^2 u(y,t)}{\partial y^2} - \frac{\rho}{\mu}\frac{\partial u(y,t)}{\partial t} = -\frac{1}{\mu}(Ae^{int} + P_0). \quad (18)$$

Here $u(y,t)$ is the sum of the velocity solutions for purely oscillatory and purely constant pressure gradients, i.e.,

$$u(y,t) = u_{osc} + u_{steady}, \quad (19)$$

where u_{osc} and u_{steady} denote the velocity solutions corresponding to oscillatory and constant pressure gradients respectively; that is, u_{osc} and u_{steady} satisfy

unsteady oscillatory flow:

$$\frac{\partial^2 u_{osc}}{\partial y^2} - \frac{\rho}{\mu}\frac{\partial u_{osc}}{\partial t} = -\frac{1}{\mu}Ae^{int}, \quad (20)$$

and

steady flow:

$$\frac{\partial^2 u_{steady}}{\partial y^2} = -\frac{1}{\mu}P_0. \quad (21)$$

The addition of steady and unsteady solutions is only legitimate when a linear form of the Navier–Stokes equation [such as eqns (3) and (18)] is valid. A general warning has been made by Goldschmied (1974), that the nonlinearities of the (full) Navier–Stokes equations preclude simple addition of steady and unsteady solutions under many conditions, e.g., if the magnitude of the steady flow component is sufficiently large. The range of conditions for which simple addition of steady and non-steady components is a valid approximation has been empirically addressed for flow inside a cylinder (Goldschmied, 1974; Fei *et al.*, 1990): simple addition of the unsteady and steady components was valid for $Re < 20000$ (based on maximum velocity) and $Wo < 45$, when the amplitude of the steady component was as large as the amplitude of the unsteady flow component [Wo calculated from reported "Stokes number" in Goldschmied (1974) and reported as "α" in Fei *et al.* (1990)]. Watson (1983) and Joshi *et al.* (1983) also give evidence for the additive effects of the steady and unsteady components of longitudinal mass transfer for one-dimensional flow in circular and rectangular channels $(1 < Wo < 8)$.

When the steady and unsteady flow components can be considered simply additive, the average flow rate (= steady component) can simply be predicted from the average pressure gradient (= steady component) (because the average of the sinusoidal unsteady component will be zero). Thus, in response to the opening question of when is it safe to ignore the unsteady nature of flow, the answer is that the unsteadiness of the flow will reflect the unsteadiness of the driving pressure gradient when $Wo < 1$, and that the flow will be less and less unsteady as Wo exceeds 1 in magnitude (the normalized amplitude of the fluid oscillations will diminish). Furthermore, whether Wo is greater or less than one in magnitude, the time-averaged flow may still be safely predicted from the time-averaged pressure gradient as if steady-state conditions exist, as long as the assumptions upon which the analysis is based are approximately satisfied. This means that any physiological process that is a function (at least primarily) of the average volume flow rate will also be independent of Wo and for these processes any oscillations may be functionally invisible. It is only those processes that scale nonlinearly with (instantaneous) flow rate that will experience an average effect that differs from that developed by a constant flow rate of the same average magnitude. Exchange processes (exchange of heat, mass, or force production) often have a nonlinear relationship with flow rate, but because the scaling factors are dependent on the range of parameters (or the magnitudes of the relevant dimensionless numbers) there will usually exist some size and velocity scales within which oscillations will be functionally neutral and other size and velocity ranges where oscillations will have a tremendous functional effect.

An example of a case where the steady and unsteady flow components are not believed to be additive is in the case of fast blood flow in large vessels (where the flow is not one-dimensional); in this case the average wall shear stress in highly oscillating flow would not be expected to be the same as the wall shear stress in a steady flow with the same mean flow rate (Pedley, 1995).

OTHER APPLICATIONS OF WO

The transition in fluid behavior at $Wo \approx 1$ discussed in detail above for cases of one-dimensional oscillatory internal flow is not the only kind of biologically-significant unsteady fluid behavior identified by the magnitude of Wo. For example, another fluid mechanical behavior that is a function of Wo is "streaming." Streaming (also called "acoustic streaming" or "secondary flow") is the formation of pockets of *steady* circulating fluid that develop in proximity to a surface when that surface is oscillating with respect to a fluid (either the fluid or the solid can be oscillating with respect to the observer, and streaming develops whether the object is flat or curved and whether the flow is internal or external as long as there is a two-dimensional

component to the flow) (Stuart, 1966; Wang, 1968; Schlichting, 1979; Sobey, 1983; White, 1991). These patterns result in net flow at points within these areas of circulation, even if the oscillating body itself has no net movement (averaged over time). Although it is clear that the details of streaming (such as the size, number and location of circulating cells) are a function of object shape, Re, and Wo (Merkli & Thomann, 1975; Nishimura et al., 1989; Tatsuno & Bearman, 1990), the critical magnitudes of Re and Wo below which streaming is less likely do not seem to be available in the literature in a form that can be easily applied (e.g. the magnitude of the streaming component is reported in differential form). Thus, we are unable to provide limits for Re and Wo below which streaming will not occur for representative geometries, but clearly the lower the magnitudes for both Re and Wo, the less likely streaming will be. In a review of the streaming literature, Wang (1968) indicates that streaming will be negligible when Wo is less than one in order of magnitude (arbitrary geometry). In a biological study, Humphrey et al. (1993) suggest that steady streaming is expected to be negligibly small adjacent to filiform hairs ($\approx 10\ \mu m$ diameter) on spider legs in response to the oscillation of air produced by motions of a nearby insect, but that streaming is possible in principle around the spider leg as a whole or around other larger cylindrical structures such as cricket cerci. In general the biological occurrence and physiological significance of streaming remains to be determined.

When the general (primarily engineering) literature on unsteady flow for a variety of geometries is examined, dimensionless groupings similar to Wo appear in solutions to transport problems (transport of mass, heat, or momentum) although there is a lack of conformity in their definitions and usage (Table 1 and other examples throughout this paper). For example, Nishimura et al. (1989) use $Wo = 4$ as a transition point in fluid behavior but their "Wo" is equivalent to $Wo^2/2\pi$ as usually defined (see Table 1). Note also that in some cases the characteristic length used to compute Wo lies within the fluid (e.g. internal flow, external flow adjacent to a flat plate) and in other cases the characteristic length lies outside the fluid (e.g. external flow around a cylinder where L refers to its diameter), which complicates comparisons between cases (as occurs for other dimensionless numbers). Despite these points, clearly the magnitude of Wo indicates significant aspects of unsteady fluid behavior, and their corresponding influence on transport processes, in a variety of cases including both external and internal flow and curved or flat surfaces. However, the identification of $Wo = 1$ as an

Table 1
Examples of Womersley-like dimensionless numbers

Parameter	Referred to as	Remarks	Geometry	Reference
$\alpha = L(n/4v)^{0.5}$		Wo (original)	flow inside circular cylinder	Womersley (1955)
$\beta = v/(nL^2)$		$1/(2Wo)^2$	flow around circular cylinder	Stuart (1966)
$N_{vib} = L^2n/v$	vibration number	$4Wo^2$	flow around sphere	Al Taweel & Landau (1976)
$\eta = L(n/8v)^{0.5}$		$Wo/(2)^{0.5}$	flow near oscillating flat plate ("Stokes' 2nd problem")	Schlichting (1979)
$\alpha = L(n/4v)^{0.5}$	Womersley number	Wo	flow between 2 flat plates	Kurzweg (1985)
$\beta = L^2n/(2\pi v)$		$2Wo^2/\pi$	flow around circular cylinder	Sarpkaya (1986)
$L(n/8v)^{0.5}$		$Wo/(2)^{0.5}$	oscillating fluid near flat plate	Denny (1988)
L^2n/v		$4Wo^2$	flow in a packed bed (around spheres)	Condoret et al. (1989)
$\alpha^2 = nL^2/(8\pi v)$	Womersley number	$Wo^2/(2\pi)$	flow between wavy-walled channels	Nishimura et al. (1989)
$\beta = L^2n/(2\pi v)$	Stokes number	$2Wo^2/\pi$	flow around circular cylinder	Tatsuno & Bearman (1990)
$R_w = L^2n/v$	Reynolds number related to the angular frequency	$4Wo^2$	flow between 2 parallel disks	Wang et al. (1990)
$(2\pi\beta)^{0.5} = L(n/4v)^{0.5}$	Womersley number	Wo	flow inside distensible tube	Zagzoule et al. (1991)
$\lambda = L(n/8v)^{0.5}$	Stokes parameter	$Wo/(2)^{0.5}$	flow inside tube	Choi & Wroblewski (1993)
$Re_SSt_S = L^2n/4v$		Wo^2	flow around circular cylinder	Humphrey et al. (1993)
$M = L(n/8v)^{0.5}$	pulsation frequency parameter	$Wo/(2)^{0.5}$	flow through porous media	Kim et al. (1994)

Nomenclature changed from original references to the following to facilitate comparisons: L is diameter of cylinder or sphere, distance between two parallel plates, or twice the distance from a single plate (m); n is angular frequency (radians s^{-1}) ($= 2\pi f$ where f is frequency in Hz); v is kinematic viscosity (m^2 s^{-1}).

approximate limit for the quasi-steady behavior of internal flow may not be applied arbitrarily for other geometries and boundary conditions nor for other unsteady fluid behaviors influenced by the magnitude of Wo.

REFERENCES

AL TAWEEL, A. M. & LANDAU, J. (1976). Mass transfer between solid spheres and oscillating fluids. A critical review. *Can. J. Chem. Engin.* **54**, 533–539.

ALTNER, H. & PRILLINGER, L. (1980). Ultrastructure of invertebrate chemo-, thermo-, and hygroreceptors and its functional significance. *Int. Rev. Cytol.* **67**, 69–139.

ATEMA, J. (1985). Chemoreception in the sea: adaptations of chemoreceptors and behavior to aquatic stimulus conditions. *Soc. Exp. Biol. Symp.* **39**, 387–423.

ATEMA, J. (1987). Temporal aspects of chemical stimuli: natural stimulus distributions, receptor cell adaptation, and behavioral function. In: *Olfaction and Taste IX. Annals of the New York Academy of Sciences*, vol. 510 (Roper, S. D. & Atema, J., eds), pp. 130–132. New York: New York Academy of Sciences.

ATEMA, J. (1988). Distribution of chemical stimuli. In: *Sensory Biology of Aquatic Animals* (Atema, J., Fay, R. R., Popper, A. N. & Tavolga, W. N., eds), pp. 29–56. New York: Springer-Verlag.

CAMHI, J. M. (1984). Auditory worlds. In: *Neuroethology: Nerve Cells and the Natural Behavior of Animals*, pp. 157–210. Sunderland: Sinauer Associates, Inc.

CARO, C. G., PEDLEY, T. J., SCHROTER, R. C. & SEED, W. A. (1978). *The Mechanics of the Circulation*. Oxford: Oxford University Press.

CHOI, Y. & WROBLEWSKI, D. E. (1993). Visualization of transition to turbulence in oscillatory flow through a rigid cast model of the central airways. *Adv. Bioeng.* **26**, 169–172.

CHRISTENSEN, T. A. & HILDEBRAND, J. G. (1988). Frequency coding by central olfactory neurons in the sphinx moth *Manduca sexta*. *Chem. Senses* **13**, 123–130.

CONDORET, J. S., RIBA, J. P. & ANGELINO, H. (1989). Mass transfer in a particle bed with oscillating flow. *Chem. Engng Sci.* **44**, 2107–2111.

COOPER, W. E. (1994). Chemical discrimination by tongue-flicking in lizards: a review with hypotheses on its origin and its ecological and phylogenetic relationships. *J. Chem. Ecol.* **20**, 439–487.

DANIEL, T. L. (1984). Unsteady aspects of aquatic locomotion. *Am. Zool.* **24**, 121–124.

DANIEL, T. L., KINGSOLVER, J. G. & MEYHOFER, E. (1989). Mechanical determinants of nectar feeding energetics in butterflies: muscle mechanics, feeding geometry,and functional equivalence. *Oecologia* **79**, 66–75.

DENNY, M. W. (1988). *Biology and the Mechanics of the Wave-swept Environment*. Princeton: Princeton University Press.

DENNY, M. W. (1993). *Air and Water: The Biology and Physics of Life's Media*. Princeton: Princeton University Press.

DENTON, E. J. & GRAY, J. A. B. (1989). Some observations on the forces acting on neuromasts in fish lateral line canals. In: *The Mechanosensory Lateral Line: Neurobiology and Evolution* (Coombs, S., Görner, P. & Münz, H., eds), pp. 229–246. New York: Springer-Verlag.

DESIMONE, J. A. (1981). Physicochemical principles in taste and olfaction. In: *Biochemistry of Taste and Olfaction*, pp. 213–229. New York: Academic Press.

DUSENBERY, D. B. (1992). *Sensory Ecology; How Organisms Acquire and Respond to Information*. New York: W.H. Freeman.

ELLINGTON, C. P. (1984). The aerodynamics of flapping animal flight. *Am. Zool.* **24**, 95–105.

ELLIS, A. G. & SMITH, D. G. (1983). Edema formation and impaired O_2 transfer in Ringer-perfused gills of the eel, *Anguilla australis*. *J. Exp. Zool.* **227**, 371–380.

FEI, D.-Y., KRAFT, K. A. & FATOUROS, P. P. (1990). Model studies of unsteady flow using magnetic resonance imaging. *J. Biomechanical Engr.* **112**, 93–99.

FLETCHER, N. H. (1992). *Acoustic Systems in Biology*. New York: Oxford University Press.

FOX, R. W. & MCDONALD, A. T. (1978). *Introduction to Fluid Mechanics*, 2nd Edn. New York: John Wiley & Sons.

FUNG, Y. C. (1997). *Biomechanics: Circulation*, 2nd Edn. New York: Springer-Verlag.

GHIRADELLA, H. T., CASE, J. F. & CRONSHAW, J. (1968). Structure of aesthetascs in selected marine and terrestrial decapods: chemoreceptor morphology and environment. *Am. Zool.* **8**, 603–621.

GLEESON, R. A., CARR, W. E. S. & TRAPIDO-ROSENTHAL, H. G. (1993). Morphological characteristics facilitating stimulus access and removal in the olfactory organ of the spiny lobster, *Panulirus argus*: insight from the design. *Chem. Senses* **18**, 67–75.

GOLDSCHMIED, F. R. (1974). Experimental study of pulsating viscous incompressible flow in rigid pipes. In: *Flow: Its Measurement and Control in Science and Industry*, vol. 1 (Dowdell, R. B., ed.), pp. 185–195. New York: Instrument Society of America.

HAHN, I., SCHERER, P. W. & MOZELL, M. M. (1994). A mass transport model of olfaction. *J. theor. Biol.* **167**, 115–128.

HAPPEL, J. & BRENNER, H. (1965). *Low Reynolds Number Hydrodynamics*. Englewood Cliffs, NJ: Prentice Hall.

HARA, T. J. (1975). Olfaction in fish. *Prog. Neurobiol.* **5**, 271–335.

HOLETON, G. F. & JONES, D. R. (1975). Water flow dynamics in the respiratory tract of the carp (*Cyprinus carpio* L.). *J. Exp. Biol.* **63**, 537–549.

HUGHES, G. M. (1966). The dimensions of fish gills in relation to their function. *J. Exp. Biol.* **45**, 177–195.

HUGHES, G. M. (1984). General anatomy of the gills. In: *Fish Physiology*, vol. 10A (Hoar, W. S. & Randall, D. J., eds), pp. 1–72. Orlando: Academic Press, Inc.

HUMPHREY, J. C., DEVARAKONDA, R., IGLESIAS, I. & BARTH, F. G. (1993). Dynamics of arthropod filiform hairs. I. Mathematical modelling of the hair and air motions. *Phil. Trans. Roy. Soc. London B* **340**, 423–444.

INOUCHI, J., SHIBUYA, T., MATSUZAKI, O. & HATANAKA, T. (1987). Distribution and fine structure of antennal olfactory sensilla in Japanese dung beetles, *Geotrupes auratus* Mtos. (Coleoptera: Geotrupidae) and *Copris pecuarius* Lew. (Coleoptera: Scarabaeidae). *Int. J. Insect Morphol. Embryol.* **16**, 177–187.

JOSHI, C. H., KAMM, R. D., DRAZEN, J. M. & SLUTSKY, A. S. (1983). An experimental study of gas exchange in laminar oscillatory flow. *J. Fluid Mech.* **133**, 245–254.

KAPOOR, N. N. (1985). External morphology and distribution of the antennal sensilla of the stonefly, *Paragnetina media* (Walker) (Plecoptera: Perlidae). *Int. J. Insect Morphol. Embryol.* **14**, 273–280.

KIM, S. Y., KANG, B. H. & HYUN, J. M. (1994). Heat transfer from pulsating flow in a channel filled with porous media. *Int. J. Heat Mass Transfer* **37**, 2025–2033.

KLEEREKOPER, H. (1969). *Olfaction in Fishes*. Bloomington: Indiana University Press.

KOEHL, M. A. R. (1996). Small-scale fluid dynamics of olfactory antennae. *Mar. Fresh. Behav. Physiol.* **27**, 127–141.

KURZWEG, U. H. (1985). Enhanced heat conduction in oscillating viscous flows within parallel-plate channels. *J. Fluid Mech.* **156**, 291–300.

KURZWEG, U. H., LINDGREN, E. R. & LOTHRUP, B. (1989). Onset of

turbulence in oscillating flow at low Womersley number. *Phys. Fluids A* **1**, 1972–1975.

LANDAU, L. D. & LIFSHITZ, E. M. (1959). *Fluid Mechanics*. Reading, MA: Pergamon Press.

MACRIDES, F. & CHOROVER, S. L. (1972). Olfactory bulb units: activity correlated with inhalation cycles and odor quality. *Science* **175**, 84–87.

McDONALD, D. A. (1955). The relation of pulsatile pressure to flow in arteries. *J. Physiol.* **127**, 533–552.

McMAHON, T. A. & BONNER, J. T. (1983). *On Size and Life*. New York: W. H. Freeman.

MERKLI, P. & THOMANN, H. (1975). Transition to turbulence in oscillating pipe flow. *J. Fluid Mech.* **68**, 567–575.

MURRAY, J. D. (1977). Reduction of dimensionality in diffusion processes: antenna receptors of moths. In: *Lectures on Nonlinear-differential-equation Models in Biology*, pp. 83–127. Oxford: Oxford University Press.

NEREM, R. M. & SEED, W. A. (1972). An *in vivo* study of aortic flow disturbances. *Cardiovasc. Res.* **6**, 1–14.

NEVITT, G. A. (1991). Do fish sniff? A new mechanism of olfactory sampling in pleuronectid flounders. *J. Exp. Biol.* **157**, 1–18.

NISHIMURA, T., ARAKAWA, S., MURAKAMI, S. & KAWAMURA, Y. (1989). Oscillatory viscous flow in symmetric wavy-walled channels. *Chem. Engng Sci.* **44**, 2137–2148.

OLSON, D. M. & ANDOW, D. A. (1993). Antennal sensilla of female *Trichogramma nubilale* (Ertle and Davis) (Hymenoptera: Trichogrammatidae) and comparisons with other parasitic Hymenoptera. *Int. J. Insect Morphol. Embryol.* **22**, 507–520.

PAYNE, T. L., MOECK, H. A., WILLSON, C. D., COULSON, R. N. & HUMPHREYS, W. J. (1973). Bark beetle olfaction. II. Antennal morphology of sixteen species of Scolytidae (Coleoptera). *Int. J. Insect Morphol. Embryol.* **2**, 177–192.

PEDLEY, T. J. (1995). High Reynolds number flow in tubes of complex geometry with application to wall shear stress in arteries. In: *Biological Fluid Dynamics* (Ellington, C. P. & Pedley, T. J., eds), pp. 219–241. Cambridge: The Company of Biologists, Limited.

PEDLEY, T. J., SCHROTER, R. C. & SUDLOW, M. F. (1977). Gas flow and mixing in airways. In: *Bioengineering Aspects of the Lung* (West, J. B., ed.). New York: Marcel Dekker, Inc.

PENNYCUICK, C. J. (1992). *Newton Rules Biology; A Physical Approach to Biological Problems*. Oxford: Oxford University Press.

PIIPER, J. & SCHEID, P. (1984). Model analysis of gas transfer in fish gills. In: *Fish Physiology*, Volume 10: *Gills. Part A. Anatomy, Gas Transfer, and Acid-Base Regulation*, pp. 229–262. Orlando: Academic Press, Inc.

RANDALL, D. & DAXBOECK, C. (1984). Oxygen and carbon dioxide transfer across fish gills. In: *Fish Physiology*, vol. 10A (Hoar, W. S. & Randall, D. J., eds), pp. 263–314. New York: Academic Press.

SARPKAYA, T. (1986). Force on a circular cylinder in viscous oscillatory flow at low Keulegan-Carpenter numbers. *J. Fluid Mech.* **165**, 61–71.

SCHLICHTING, H. (1979). *Boundary-Layer Theory*, 7th Edn. New York: McGraw-Hill.

SCHMITT, B. C. & ACHE, B. W. (1979). Olfaction: responses of a decapod crustacean are enhanced by flicking. *Science* **205**, 204–206.

SCHNEIDER, D. (1964). Insect antennae. *Ann. Rev. Entomol.* **9**, 103–122.

SCHWENK, K. (1994). Why snakes have forked tongues. *Science* **263**, 1573–1577.

SOBEY, I. J. (1983). The occurrence of separation in oscillatory flow. *J. Fluid Mech.* **134**, 247–257.

STUART, J. T. (1966). Double boundary layers in oscillatory viscous flow. *J. Fluid Mech.* **24**, 673–687.

TATSUNO, M. & BEARMAN, P. W. (1990). A visual study of the flow around an oscillating circular cylinder at low Keulgan-Carpenter numbers and low Stokes numbers. *J. Fluid Mech.* **211**, 157–182.

VAN DER PERS, J. N. C., CUPERUS, P. L. & DEN OTTER, C. J. (1980). Distribution of sense organs on male antennae of small ermine

moths, *Yponomeuta* spp. (Lepidoptera: Yponomeutidae). *Int. J. Insect Morphol. Embryol.* **9**, 15–23.

VOGEL, S. (1992). *Vital Circuits: On Pumps, Pipes, and the Workings of Circulatory Systems*. New York: Oxford University Press.

VOGEL, S. (1994a). *Life in Moving Fluids: The Physical Biology of Flow*, 2nd Edn. Princeton: Princeton University Press.

VOGEL, S. (1994b). Nature's pumps. *Am. Sci.* **82**, 464–471.

WANG, C.-Y. (1968). On high-frequency oscillatory viscous flows. *J. Fluid Mech.* **32**, 55–68.

WANG, Z., ISHIZAWA, S. & TAKAHASHI, K. (1990). Unsteady viscous flow between two parallel disks with a time-varying gap width and central fluid source (the case in which the rate of flow from the source is forcibly varied with time). *JSME Int. J.* **33**, 446–453.

WATSON, E. J. (1983). Diffusion in oscillatory pipe flow. *J. Fluid Mech.* **133**, 233–244.

WEIS-FOGH, T. (1973). Quick estimates of flight fitness in hovering animals, including novel mechanisms for lift production. *J. Exp. Biol.* **59**, 169–230.

WHITE, F. M. (1991). *Viscous Fluid Flow*. 2nd Edn. New York: McGraw-Hill.

WOMERSLEY, J. R. (1955). Method for the calculation of velocity, rate of flow and viscous drag in arteries when the pressure gradient is known. *J. Physiol.* **127**, 553–563.

ZAGZOULE, M., KHALID-NACIRI, J. & MAUSS, J. (1991). Unsteady wall shear stress in a distensible tube. *J. Biomechanics* **24**, 435–439.

APPENDIX

A	amplitude of pressure gradient oscillations, N m^{-3}
a	half of the distance between the two parallel plates, m
e	base of natural logarithm (2.718 ...)
f	frequency, cycles s^{-1}
i	$\sqrt{-1}$
$\Im$	Ifraktur; imaginary part of a complex number
L	characteristic length, m; $L = 2R$
l	length of parallel plates in x direction, m
n	frequency, radians/s; $n = 2\pi f$
p	pressure, Pa
Q	volume flow rate, m^3 s^{-1}
R	half of characteristic length, m; $R = L/2$
$\Re$	Rfraktur; real part of a complex number
Re	Reynolds number (dimensionless); $Re = LU_0/v$
St	Strouhal number (dimensionless); $St = fL/U_0$
T	period of cycle, s; $T = 1/f$
t	time, s
u	velocity component in x direction, m s^{-1}
U_0	characteristic velocity used to calculate dimensionless numbers, m s^{-1}
Wo	Womersley number (dimensionless); $Wo = 0.5L(n/v)^{0.5}$
μ	dynamic viscosity of fluid, kg (m s)$^{-1}$
v	kinematic viscosity of fluid, m^2 s^{-1}; $v = \mu/\rho$
ρ	density of fluid, kg m^{-3}